Molecular Therapy
Methods & Clinical Development
Original Article

Optogenetic targeting of AII amacrine cells restores retinal computations performed by the inner retina

Hanen Khabou,[1,2] Elaine Orendorff,[1,2] Francesco Trapani,[1,2] Marco Rucli,[1] Melissa Desrosiers,[1] Pierre Yger,[1] Deniz Dalkara,[1,3] and Olivier Marre[1,3]

[1]Sorbonne Université, INSERM, CNRS, Institut de la Vision, 17 rue Moreau, 75012 Paris, France

Most inherited retinal dystrophies display progressive photoreceptor cell degeneration leading to severe visual impairment. Optogenetic reactivation of inner retinal neurons is a promising avenue to restore vision in retinas having lost their photoreceptors. Expression of optogenetic proteins in surviving ganglion cells, the retinal output, allows them to take on the lost photoreceptive function. Nonetheless, this creates an exclusively ON retina by expression of depolarizing optogenetic proteins in all classes of ganglion cells, whereas a normal retina extracts several features from the visual scene, with different ganglion cells detecting light increase (ON) and light decrease (OFF). Refinement of this therapeutic strategy should thus aim at restoring these computations. Here we used a vector that targets gene expression to a specific interneuron of the retina called the AII amacrine cell. AII amacrine cells simultaneously activate the ON pathway and inhibit the OFF pathway. We show that the optogenetic stimulation of AII amacrine cells allows restoration of both ON and OFF responses in the retina, but also mediates other types of retinal processing such as sustained and transient responses. Targeting amacrine cells with optogenetics is thus a promising avenue to restore better retinal function and visual perception in patients suffering from retinal degeneration.

INTRODUCTION

Blindness affects 45 million people worldwide. In many cases of retinal degeneration photoreceptors are lost, while retinal ganglion cells (RGCs) (that provide visual signals to the brain) as well as many interneurons (e.g., amacrine cells) are maintained. This opens the possibility to stimulate the remaining RGCs or amacrine cells directly to restore visual function. Retinal prostheses are a promising solution and have been found to restore some useful perception in blind patients. However, the acuity of the existing devices remains very low, below the level of legal blindness.[1,2] Patients also report that percepts evoked by electrical stimulation of retinal neurons are not easily interpretable as visual stimuli[3] and therefore are often not sufficient to identify objects or to navigate in complex environments. Optogenetic therapies provide a promising alternative to restore vision with a higher resolution and specificity that can better mimic the natural output of the retina.[4] In this strategy, a light-sensitive protein is expressed in specific neural populations in a blind retina.

Expressing light-sensitive proteins in RGCs can be an efficient way to restore vision through the stimulation of these newly light-sensitive cells with patterned light to evoke visual perception,[5–9] although the first results show that the acuity is still low with this strategy.[10] How to optimize visual acuity and perceptual performance when restoring vision using optogenetics is an active area of investigation.

In a healthy retina, the ganglion cell population can be divided into about 20–40 cell types that each perform a different computation on the visual scene.[11,12] Each cell type is classically assumed to be selective of a specific feature of the visual scene and therefore conveys a corresponding feature map to the brain.[13] Altering specifically one of these cell type populations can lead to specific impairments in visual perception and motor output, including specific defects in perceiving moving objects and eye movement control.[14–16] In particular, ganglion cells usually respond either to light increase (ON ganglion cells) or light decrease (OFF ganglion cells). Inactivating ON ganglion cells leads to a reduced ability to detect increase of luminance at the perceptual level while ability to detect decrease of luminance is not affected.[17] Optogenetic strategies targeting ganglion cells will not restore the computations performed in the normal retina. In particular, making ganglion cells light-sensitive will result in a retina where all ganglion cells become de facto ON cells (only responding to light increase). It is unclear how this synthetic visual signal will affect the physiological processing performed by downstream areas in the brain and what will be the resulting restored perception, but this loss of retinal computations could severely impair perceptual performance.

To restore some of the response diversity found in normal retinas with optogenetic therapy, other cells such as "dormant" photoreceptors have been targeted specifically.[18] However, in many patients these cells have already been lost due to retinal degeneration. An

Received 28 July 2023; accepted 8 September 2023;
https://doi.org/10.1016/j.omtm.2023.09.003.

[2]These authors contributed equally

[3]These authors contributed equally

Correspondence: Olivier Marre, Sorbonne Université, INSERM, CNRS, Institut de la Vision, 17 rue Moreau, 75012 Paris, France.
E-mail: olivier.marre@inserm.fr

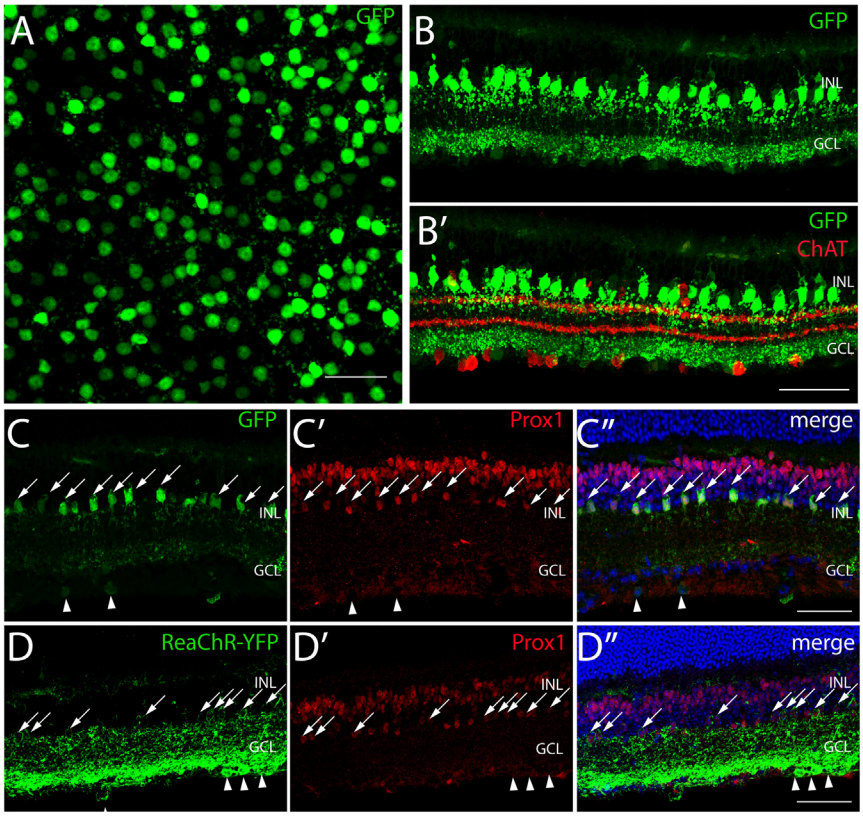

Figure 1. AAV-mediated gene delivery to AII amacrine cells from the vitreous

(A) Whole-mount view showing eGFP expression (green) in the plane of AII somas (INL). (B) Retinal cryosections showing eGFP expression (green) and labeling of starburst amacrine cells with a ChAT antibody (red). (C, C′, C″) Retinal cryosections showing eGFP expression under the control of our HKamac sequence (in green) and Prox1 immunostaining (in red) (and DAPI in blue). (D, D′, D″) Retinal cryosections showing ReaChR-eYFP expression under the control of our HKamac sequence (in green), Prox1 immunostaining (in red) and DAPI in blue). For all panels, retinal layers are shown on the left: inner nuclear layer (INL), ganglion cell layer (GCL). DAPI labels all nuclei, while Prox1 labels bipolar and AII amacrine cells. Co-labeled AII amacrine cells are indicated with white arrows. Co-labeled RGCs are indicated by white arrowheads. Scale bars, 50 μm.

alternative strategy to restore richer functional selectivity is to target other cell types in the intermediate layers of the retina that are not damaged. Here, we express an optogenetic protein in AII amacrine cells of blind mice to restore vision. AII amacrine cells are an ideal target because they connect with both ON and OFF bipolar cells with different types of synapses.[19–23] They form gap junctions with most ON bipolar cell types,[24] and can therefore excite them when they are activated. At the same time, they form glycinergic inhibitory synapses with most OFF bipolar cell types.[24–26]

We first introduce a vector allowing to target specifically AII amacrine cells, enabling expression of an optogenetic protein following an AAV injection. We then show that this strategy allows reactivating retinal computations, and in particular ON-OFF selectivity, in a way similar to the normal retina. We demonstrate this both in normal retinas where photoreceptor transmission is blocked and in a model of retinal degeneration where photoreceptors have been lost. Our data show that targeting AII amacrine cells is a promising strategy for vision restoration with optogenetics.

RESULTS

Targeting of AII amacrine cells

To identify a sequence driving expression in AII amacrine cells, we generated plasmid constructs with several known retinal-specific promoters, encoding eGFP expression. Then, we produced AAV vectors with the corresponding expression cassettes and tested the resulting expression pattern, via intravitreal injection route with AAV2-7m8, a genetic variant of AAV2[27,28] specifically selected for enhanced retinal transduction properties when delivered intravitreally. We incidentally found a sequence driving specific expression in AII amacrine cells. The regulatory cassette, that we refer to as HKamac in the following (see Tables S1–S4), has been derived from the IRBP enhancer and the human GNAT2 promoter, previously described for weak targeting of photoreceptors,[29–33] and included an additional sequence at its 3′ end immediately after GNAT2 promoter into which an SV40 intron was inserted. C57BL/6J wild-type mice were injected at 4 weeks of age using AAV2-7m8-HKamac-eGFP. Six weeks after injection, eye fundus showed high expression levels (Figure S1). Retinas were then harvested, fixed, and embedded in tissue freezing medium for histology and immunohistochemistry analysis 120–140 days postinjection.

Wild-type retinal flat mounts showed that a homogeneous population of cells with large somas expressed GFP in the inner nuclear layer (INL) (Figures 1A and S1; Video S1). In cross-sections, the labeled cells showed dendritic stratification in both ON and OFF layers, a pattern reminiscent of AII morphology.[34] To determine precisely the subtype of amacrine cell, we first showed that GFP did not colocalize with GABAergic (GAD staining, see Figure S1B, S1B′) or with Starburst amacrine cell marker (ChAT staining) (Figure 1B). To determine whether they were glycinergic AII amacrine cells, we performed cryosections labeling with a Prox1 antibody, labeling both glycinergic bipolar cells and AII amacrine cells,[35] and found clear co-localization of GFP with Prox1, thereby confirming GFP-positive cells are glycinergic AII amacrine cells (Figures 1C, 1C′, and 1C″). We then replaced GFP by ReaChR-eYFP in the plasmid construct while keeping the same regulatory sequence. ReachR-eYFP was then

delivered in wild-type mice using the same AAV2-7m8 capsid variant. ReaChR-eYFP was successfully expressed in AII amacrine cells' membranes, although eYFP was detected in some RGCs as well (Figure 1D, 1D′, and 1D″). The off-target expression pattern can depend on the viral dose and the injection route.[28] ReaChR is also very efficiently expressed which skews expression toward a broader range of cell types.

Optogenetic stimulation of AIIs produces ON and OFF responses

AII amacrine cells excite ON bipolar cells through gap junctions, and inhibit OFF bipolar cells through glycinergic, inhibitory synapses. We tested if stimulation of AII amacrine cells with optogenetics could evoke ON and OFF responses in RGCs. For this we recorded RGC spiking activity from wild-type retinas expressing ReaChR under the HKamac sequence on a multielectrode array (see Tables S1–S4 for sequence, Figure 2A). To test if AII stimulation could activate similar circuits to photoreceptor stimulation, we first measured the responses of ganglion cells to stimuli at low light intensity, which only activated photoreceptors, and were not sufficiently strong to activate ReaChR (termed photoreceptor stimulation in the following). We observed both ON and OFF responses (Figure 2B).

We then blocked the synaptic transmission from photoreceptors to the ON and OFF bipolar cells using pharmacology (L-AP4 to block the transmission from photoreceptors to ON bipolar cells, and ACET to block transmission from photoreceptors to OFF bipolar cells, see materials and methods). At the same light intensity, responses disappeared. This is expected since the impact of photoreceptor activation on the rest of the retinal circuit has been blocked, and the light intensity is too low to activate ReaChR. We then increased light intensity to reach the activation of ReaChR (see materials and methods) and observed both ON and OFF responses to light stimulation (Figures 2C and 2D) for a large portion of ganglion cells. This activation (termed optogenetic stimulation in the following) is due to the stimulation of AII since stimulation in untreated retinas at similar intensity with the same concentration of blockers did not show any response (Figure 2E). Activation of AII with optogenetic stimulation is thus able to evoke both ON and OFF responses in the retina, while previous studies showed that targeting ganglion cells only gave ON responses.[5–9,36]

To understand if our strategy allows reactivation of the same computations performed in the normal retina, we categorized the cells as ON, OFF, or ON-OFF depending on their responses to photoreceptor stimulation. ON ganglion cells were defined as responding to the onset of the photoreceptor stimulation, OFF cells as responding to the offset, and ON-OFF as responding to both (see materials and methods). We then asked if ON cells and OFF cells responded to both the onset and offset of the optogenetic stimulation. If the responses were consistent for photoreceptor and optogenetic stimulation, this would suggest that AII stimulation is able to reactivate some of the circuits that are active during photoreceptor stimulation. For example, ON ganglion cells receive their inputs from ON bipolar cells. At the onset of AII stimulation, ON bipolar cells should be activated, and should therefore stimulate ON ganglion cells. Conversely, OFF bipolar cells, which provide the main excitatory input to OFF ganglion cells, should be inhibited during AII stimulation, and uninhibited at the offset of AII stimulation. As a result, they should be able to excite OFF ganglion cells at the offset of the AII stimulation. If this hypothesis were correct, ON ganglion cells should be activated at the onset of AII stimulation, and OFF ganglion cells at the offset.

We identified a total population of 173 ON and 65 OFF (and 44 ON-OFF) ganglion cells across three different experiments. The large majority of ON cells responded to the onset of the optogenetic stimulation (74%) while their responses to the offset were almost not present (only 0.5%), which is consistent with our hypothesis. A significant portion of OFF cells showed OFF responses to the optogenetic stimulation (25%). However, we also observed that a fraction of cells classified as OFF based on response to photoreceptor stimulation, turned ON during optogenetic stimulation (36%). We hypothesized that this could be due to off-target expression of the ReachR protein in ganglion cells, observed in our histology experiments.

Off-target expression explains changes in ON-OFF selectivity

If the observed responses at the onset for OFF cells were due to direct expression of ReaChR in ganglion cells, these responses would still be present when fully blocking glutamatergic synaptic transmission. To test this, we performed additional experiments on the same cell populations where we fully blocked this transmission using a pharmacological cocktail composed of L-AP4, ACET, CNQX, and CPP (Figure 3A, see materials and methods). The responses at the stimulation onset in OFF ganglion cells were still present after the application of this cocktail (Figures 3B, 3C, and 3D): 41% of the OFF cell population responded to the stimulus onset at bright luminance, while responses to the stimulus offset completely disappeared (Figure 3E). In control retinas where no optogenetic protein is expressed, light responses were almost completely abolished (99% or the OFF population did not respond to the stimulus, Figure 3F). This confirms that these onset responses in OFF cells are due to off-target expression in ganglion cells.

This off-target expression had two consequences. First, when varying the stimulation light intensity, there were more and more ganglion cells responding to light onset when increasing light intensity (Figure S2). Our results suggest that this is due to a weaker off-target expression in ganglion cells, which require a higher intensity to reach the spike threshold. When increasing light intensity, more ganglion cells have a light response due to off-target expression. Second, ON-OFF cells, characterized with photoreceptor stimulation, usually respond to light onset for optogenetic stimulation. This might be due to off-target expression in ganglion cells: to respond to light onset, a ganglion cell can either receive ON bipolar cell output, or express ReaChR due to off-target expression. To respond to light offset, a cell has to receive OFF bipolar cell output. This asymmetry might explain why we observed fewer responses to light offset than to light onset in ON-OFF ganglion cells.

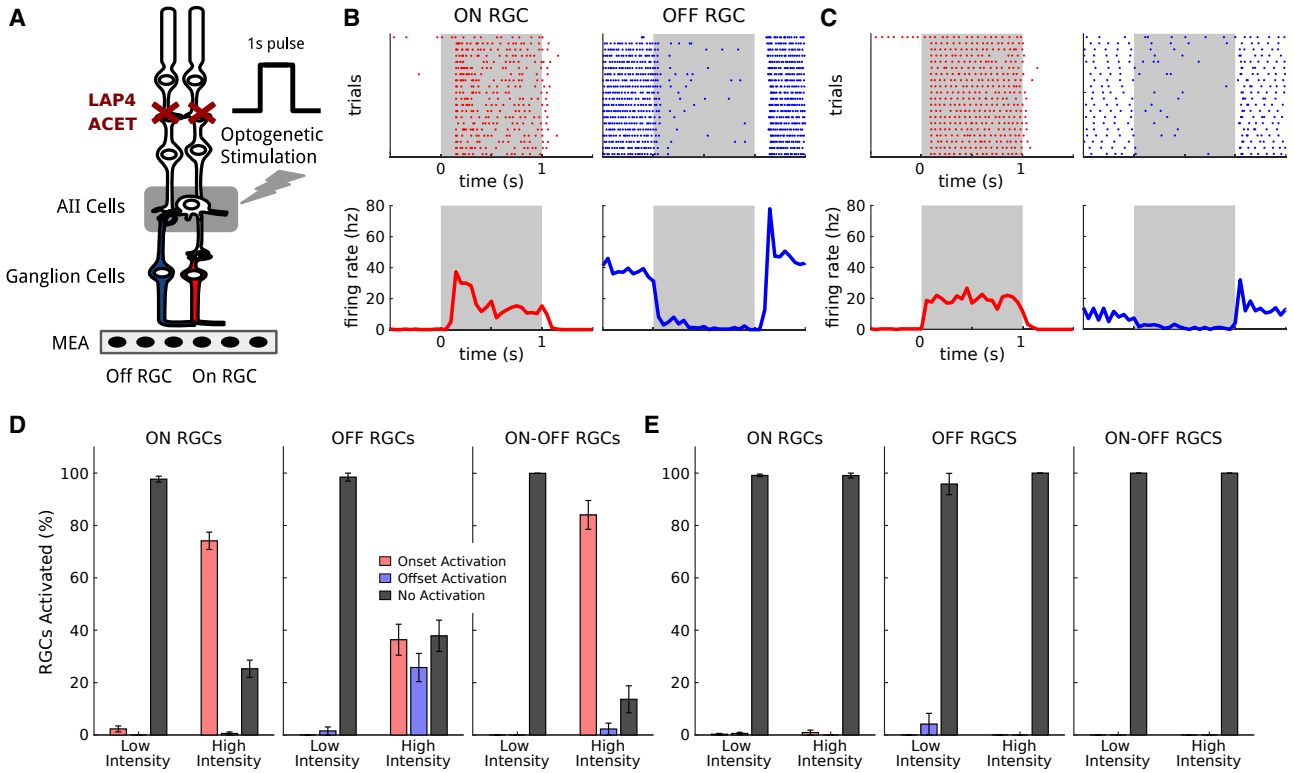

Figure 2. ON and OFF RGC responses elicited upon light stimulation of ReaChR-expressing AII amacrine cells

(A) AII amacrine cells connect to the ON pathway (in red) through gap junctions, and to the OFF pathway (in blue) through glycinergic inhibitory connections. Stimulation of AIIs hence produces responses of opposite polarity on ON and OFF RGCs. We target AIIs through optogenetic stimulation consisting of a series of full-field flashes, and record the responses of the RGCs with a multielectrode array. Pharmacology (ACET and L-AP4) blocks synaptic transmission from photoreceptors. (B) Responses of representative ON (left column, red) and OFF (right column, blue) RGCs to photoreceptor stimulation with white full-field flashes. Top: spiking activity across different trials. Bottom: mean response. The time intervals of the flashes are shown in gray. (C) Responses of the same ON (left column, red) and OFF (right column, blue) RGCs shown in (B) to optogenetic stimulation, after blocking photoreceptor synaptic transmission. Top: spiking activity across different trials. Bottom: mean response. (D) Percentage of RGCs responding to optogenetic stimulation. Left: percentage of ON RGCs responding to the flash respectively at onset (red), offset (blue), or never (black), for both low and high luminance. Center and Right: same plot for OFF and ON-OFF RGCs, respectively. Error bars represent the standard error of the sample mean. (E) Percentage of RGCs responding to optogenetic stimulation for a control population with no opsin expressed. Same plots as in (D). Error bars represent the standard error of the sample mean.

Ganglion cell ON and OFF responses can be evoked by AII stimulation

To further demonstrate that the observed responses were mostly due to AII activation and not off-target expression in ganglion cells, nor to a failure of the pharmacological blocking of photoreceptor transmission, we performed additional experiments. We reasoned that if we use an inhibitory opsin, which will hyperpolarize the cells upon light stimulation, it will inactivate ganglion cells. As a consequence, off-target expression will not allow any spiking response. On the contrary, if AII are hyperpolarized upon light stimulation, they should still evoke responses, except that they should be inverted: ON ganglion cells should respond at light offset, and OFF ganglion cells at light onset. If the responses are due to a failure of the pharmacological blocking, we should not see this inversion.

We injected the same construct but replaced ReaChR with gtACR1 (see materials and methods).[37,38] We performed the same protocols (two retinas, 36 ON, 125 OFF, and nine ON-OFF RGCs) and found that most ganglion cells for which a response was detected showed the predicted inversion of polarity (Figures 4A, 4B, and 4C). Observed responses are thus due to AII modulation, and not to off-target expression, nor to a failure of the pharmacological block. These results confirm that our approach allows stimulation of AII to modulate differentially ON and OFF ganglion cells.

Diversity of ganglion cell responses to AII stimulation

AII stimulation can restore ON and OFF responses, but can it restore more features of the normal retinal responses? In particular, beyond the ON and OFF classification, previous works on normal retinas have shown that retinal responses to more complex stimuli like "chirp" stimuli uncover a large diversity of responses, corresponding to the different types of ganglion cells. Is this diversity still present in retinas reactivated by our AII stimulation strategy? To test this, we displayed the chirp stimulus, previously used to classify different types of ganglion cells,[12] at high light intensity so that it activates

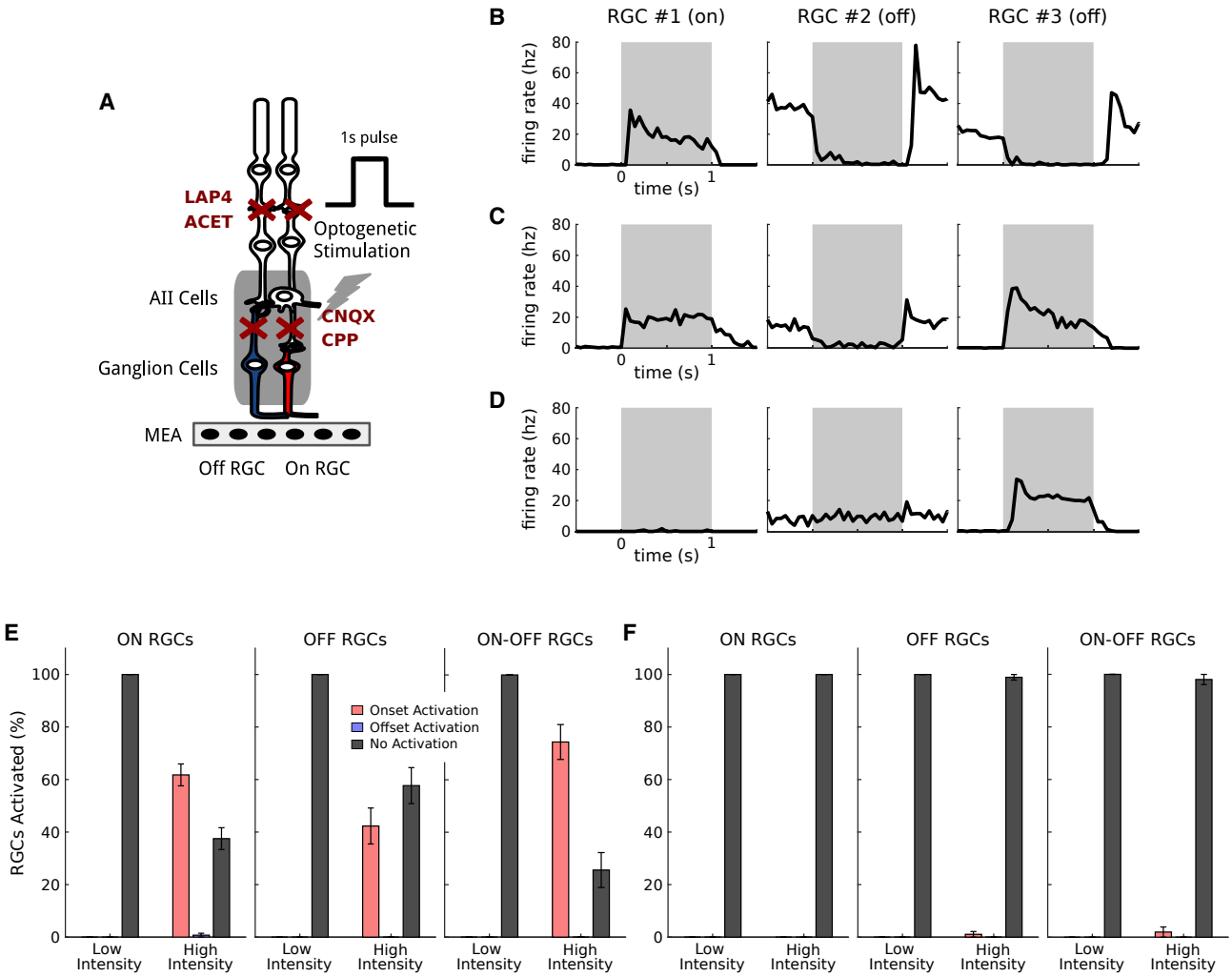

Figure 3. Off RGC responses of inverted polarity are due to off-target opsin expression

(A) Control protocol showing direct ganglion cell activation due to off-target expression of ReaChr: the application of CNQX and CPP disrupts all the excitatory synaptic connections. Responses induced by visual stimulations under this condition are only due to direct activation of the RGCs expressing the opsin. (B) Mean responses of three representative RGCs (one ON and two OFF) to simple photoreceptor stimulation. The stimulation time interval is depicted in gray. (C) Mean responses of the same three RGCs to optogenetic stimulation, after blocking the photoreceptor transmission. (D) Mean responses of the same RGCs after blocking all the excitatory synaptic connections. Responses of RGC 3 can only be explained by off-target expression of the opsin in ganglion cells. (E) Percentage of ganglion cells responding to direct optogenetic stimulation, due to off-target expression. Left: percentage of ON RGCs responding respectively to the stimulus onset or offset (or not responding), at both low and high luminance. Center and Right: same plot for OFF and ON-OFF RGCs, respectively. Error bars represent the standard error of the sample mean. (F) Percentage of ganglion cells responding to direct optogenetic stimulation for a control population with no opsin expressed. Same plots as in (E). Error bars represent the standard error of the sample mean.

the ReaChR protein expressed in AII amacrine cells. We found a large diversity of responses to this stimulus (Figure 5A). Beyond responses to onset and offset, some cells responded to different parts of this stimulus, showing different tunings to temporal frequencies.

A few cells responded transiently while most of them had more sustained responses. To quantify this, we first measured an index of how transient or sustained ganglion cell responses were (see materials and methods). We computed this index both on the responses to optogenetic stimulation and to normal photoreceptor responses: we found that a large majority of cells lost their transient component when reactivated through the AII pathway (Figure 5B). We also defined a comparative sustained-transient index that measures how transient is the response of a ganglion cell when activated optogenetically, with respect to its normal photoreceptor response (Figure 5C). An analysis of the distribution of these indices showed that ON ganglion cells are consistently more sustained in their optogenetic responses (tested with the Wilcoxon rank-sum test,

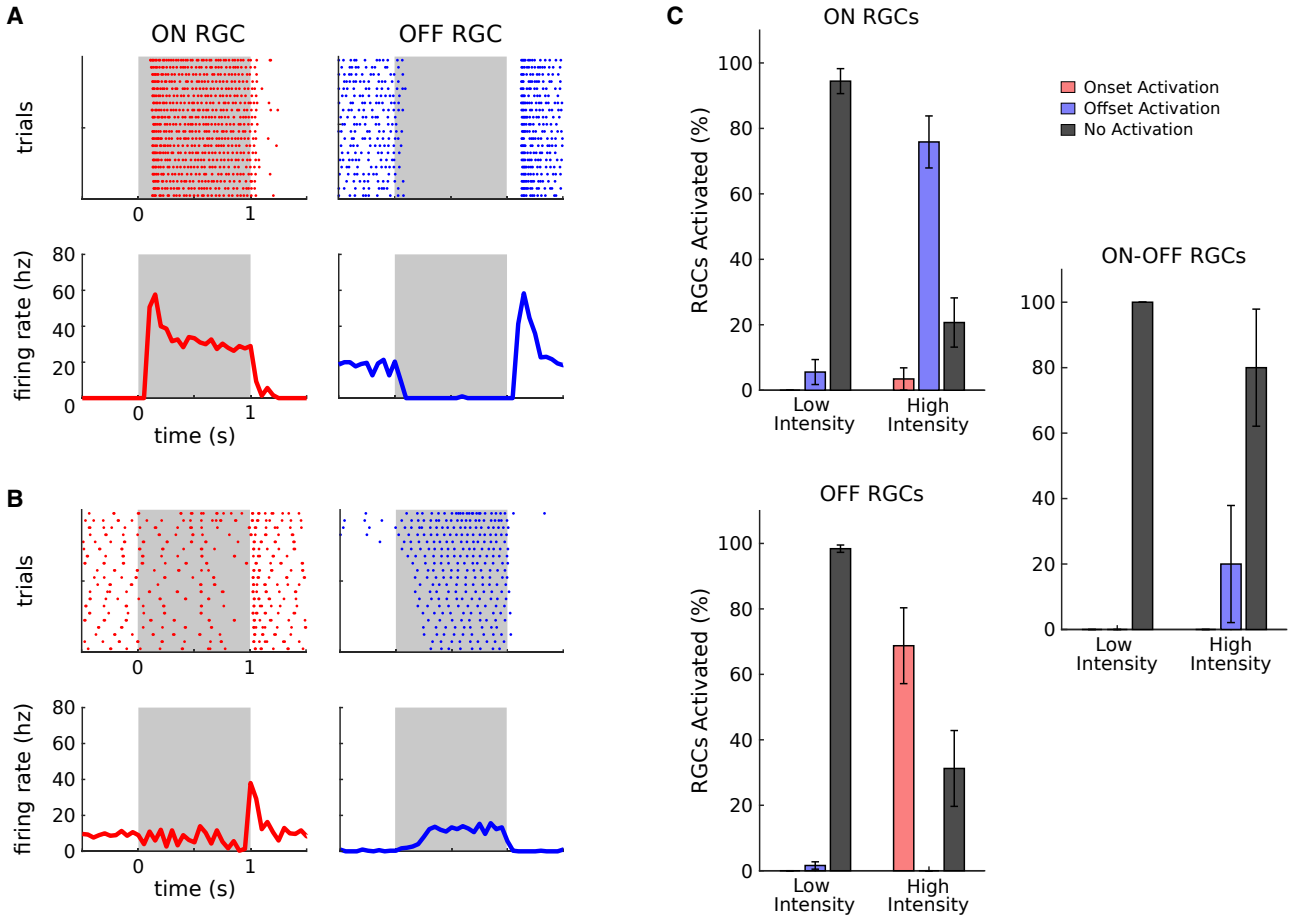

Figure 4. The diversity of RGC responses is really due to AII activation, and not to photoreceptor transmission or off-target expression

(A) Examples of responses to photoreceptor stimulation for representative ON (left column, red) and OFF (right column, blue) RGCs. Top: Raster plot of RGC responses across trials. Bottom: mean responses. The stimulation period is represented by the gray regions. (B) same as (A) for optogenetic stimulation, after blocking photoreceptor transmission: this time All amacrine cells express an inhibitory opsin, gtACR1. (C) Percentage of RGCs responding to optogenetic stimulation (with the inhibitory opsin gtACR1). Top: percentage of ON RGCs responding respectively at stimulus onset (red), stimulus offset (blue), or not responding (black), for both low and high luminance. Bottom and Right: same plot for OFF and ON-OFF RGCs, respectively. Error bars represent the standard error of the sample mean.

p value below 1e-5; see materials and methods), while the result is less clear for OFF cells.

We then checked if the optogenetic stimulation of AIIs preserved or disrupted the functional organization of RGCs. RGCs can be classified into several types: cells belonging to the same type are spatially arranged to cover uniformly the visual field, and produce similar responses to the same stimuli. To check if this organization was still present, we looked at correlations of the responses of pairs of RGCs for both photoreceptor and optogenetic stimulations (Figure 5D). If the functional arrangement is preserved in optogenetically reactivated retinas, these correlations should not vary significantly across these two conditions. We used the Pearson correlation coefficient to estimate the correlation of two cells responses. We looked at the correlations of all cell pairs with the same polarity, for both photoreceptor and optogenetics responses. We observed that for most of the ganglion cell pairs considered, these correlations were still present during optogenetic stimulation (Figure 5D).

As a further estimation of the diversity of the responses, we calculated the dimensionality of the space of possible responses. For this we performed a principal-component analysis (PCA) on the ensemble of all the ganglion cell average responses to the chirp stimulus. If all the cells responded the same way to the stimulus, the first principal component would explain all the variance in these responses. On the contrary, if all the responses were very different, it would take a lot of components to explain most of the variance. We found that, for both normal and reactivated retinas, we needed more than six components to explain more than 95% of the total variance in the response (Figure 5E). This shows that our strategy is able to restore a large part of the diversity in the visual responses.

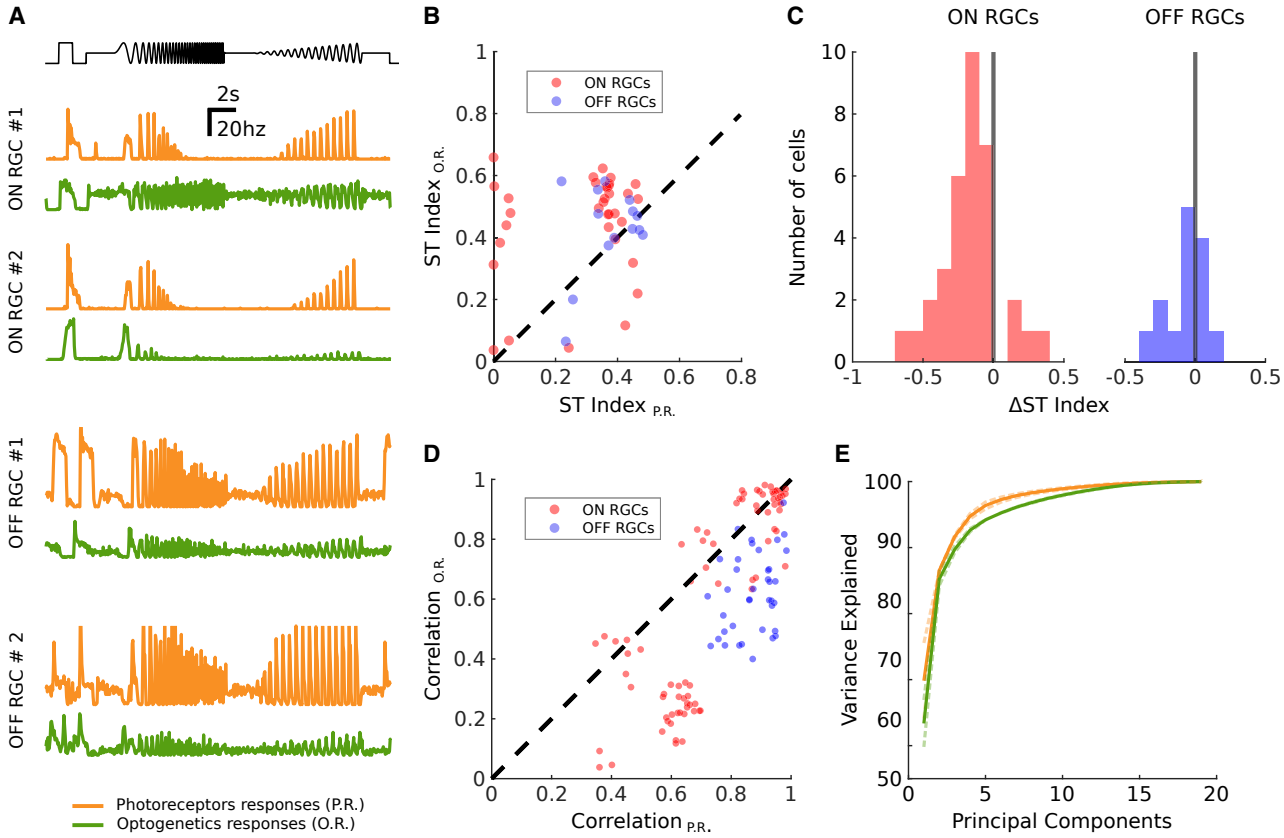

Figure 5. All activation generates diverse RGC responses

(A) On top in black: the temporal profile of the full-field chirp stimulus (luminance over time). Below: mean responses of four representative RGCs to the chirp stimulus. In orange: responses mediated by photoreceptors (no optogenetics involved). In green: responses mediated by the optogenetic activation of AIIs (with blocked photoreceptor transmission). (B) Comparison between the sustained-transient index computed on photoreceptor and optogenetic responses for 48 selected RGCs. Each dot shows the index for a different RGC, for both photoreceptor responses (x axis) and optogenetic responses (y axis). Values close to 1 mean the response is predominantly sustained; values close to zero mean the response is predominantly transient. (C) Distribution of the comparative sustained-transient index ΔST for the ON (red) and OFF (blue) RGC populations (same 48 RGCs shown in B). An index close to 1 means that the cell responds more transiently when activated optogenetically with respect to its normal photoreceptor responses. Conversely, an index close to −1 means that the optogenetic responses are more sustained than the normal photoreceptor responses. (D) Response correlations across RGC pairs from a population of 40 RGCs, for both photoreceptor and optogenetic stimulations. Pearson correlation coefficient computed on the responses of pairs of RGCs to photoreceptor stimulation (x axis) and to optogenetic stimulation (y axis). Red dots represent ON to ON response correlations: blue dots represent OFF to OFF response correlations. (E) Principal-component analysis of the mean RGC responses to the chirp stimulus for a selected population of 40 cells (same shown in D). Each curve shows the number of principal components needed (x axis) to explain a given percentage of variance in the ganglion cell responses (y axis). We show the curves for both photoreceptor responses (orange) and optogenetic responses (green). Light dashed curves represent analysis conducted on the individual experiments. Dark, continuous lines represent the average across all experiments.

All stimulation in degenerated retinas restores ON and OFF responses

So far we worked with wild-type retinas where we could compare the same ganglion cells responding to photoreceptor stimulation and optogenetic stimulation of AII amacrine cells. However, in retinal dystrophies, the retinal network is rewired following the degeneration.[39,40] Is AII stimulation still able to evoke responses after the rewiring imposed by degeneration? To test this, we performed the same experiments on rd1 mice. We obtained a similar expression pattern in rd1 mice as in wild-type mice (Figures 6A, 6B, and 6C). We recorded the retinas at the age of 3 months when there are no measurable responses to light due to photoreceptor degeneration. We collected data accounting for a total population of 160 RGCs, measured their responses to light flashes, and consistently found both ON and OFF responses (Figures 6D and 6E). This demonstrates that the rewiring of the network following degeneration does not affect the ability of our strategy to restore diverse responses in ganglion cells.

DISCUSSION

Here, we report a broadly applicable strategy that can be used to restore visual function in patients suffering from photoreceptor degeneration. We targeted, for the first time, AII amacrine cells thanks to a vector allowing high levels of microbial opsin expression

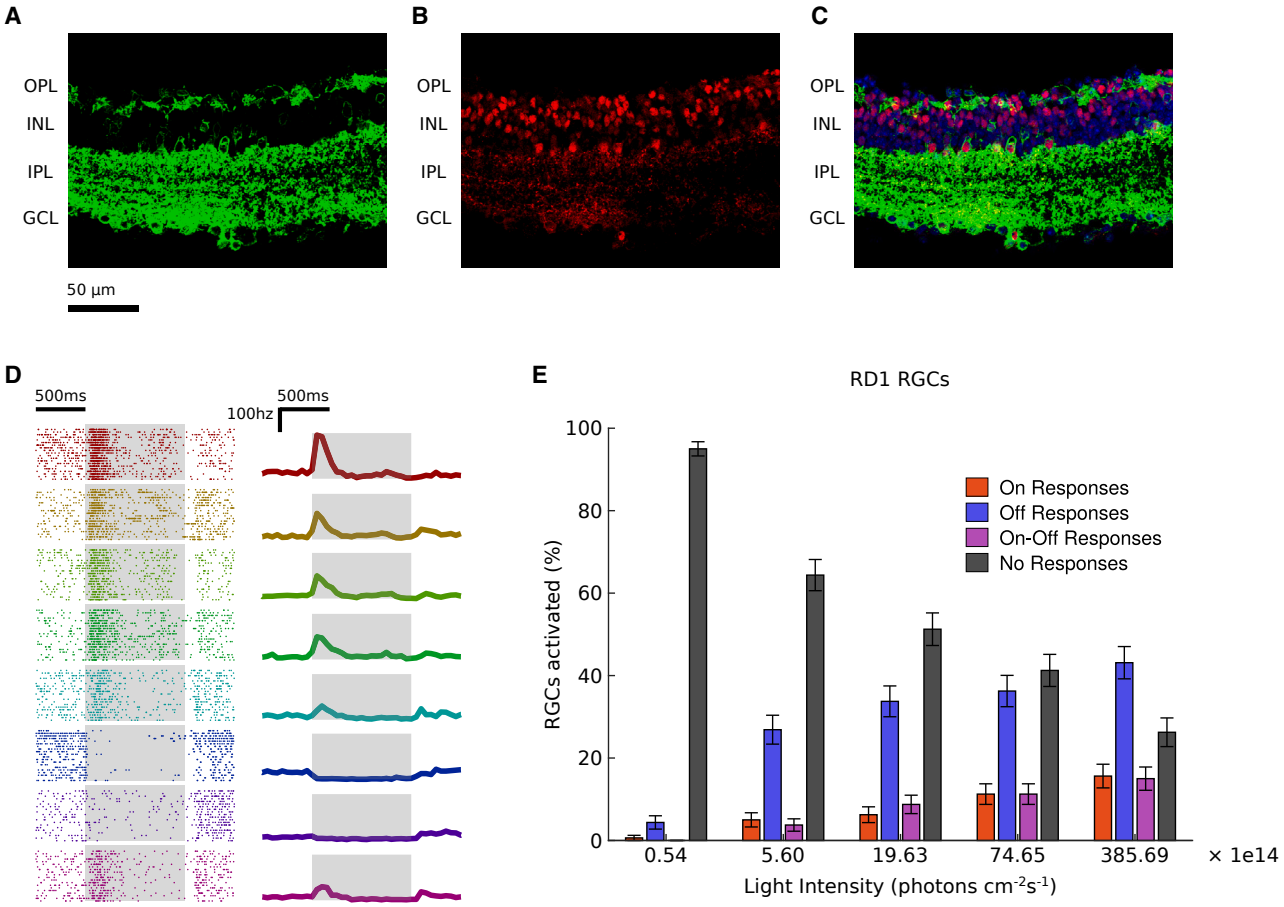

Figure 6. Optogenetic activation of AIIs produces ON and OFF RGC responses also in dystrophic retinas

(A, B, and C) Cross section of a dystrophic mouse retina (rd1) showing ReaChR-eYFP expression (green, panels A and C) under HKamac sequence; co-localization with Prox1 antibody (red, panels B and C) indicates ReaChR expression in AII amacrine cells. Expression under control of DAPI is shown in blue (C). AII amacrine cells are indicated with white arrows. Retinal layers are shown on the left: outer plexiform layer (OPL), inner nuclear layer (INL), inner plexiform layer (IPL), ganglion cell layer (GCL). (D) Optogenetic responses of 10 representative RGCs from dystrophic retinas to a series of flashes. Left: raster plots of the responses; each row (and color) represents a different cell; the stimulation period is highlighted in gray. Right: mean responses over trials. (E) Activation of RGCs in dystrophic retina due to optogenetic stimulation. For each of five luminance levels, we plot the percentage of RGCs that responded to the optogenetic stimulation with pure ON (red), pure OFF (blue), ON-OFF (magenta), or no responses (black). Error bars represent the standard error of the sample mean.

in this cell type rendering them light sensitive. Our strategy has the advantage of being mutation-independent, and can potentially be used for different genotypes of retinal dystrophies. Compared with ganglion cell targeting, which is currently in clinical trials, our approach has the advantage of restoring a significant part of the retinal computations performed by a normal retina. In particular, we have shown that this strategy allows restoration of both ON and OFF ganglion cell responses. We also observed diverse responses, presumably corresponding to the activation of several different cell types and pathways in the retinal circuit, similar to what happens in the normal retina.

The expression of channelrhodopsin2-GFP using AAV2 under a ubiquitous promoter was shown both in short-term and long-term studies for up to 18 months.[5,41] In these studies, expression of channelrhodopsin2-GFP was observed predominantly in retinal ganglion as well as in displaced amacrine cells of the ganglion cell layer. At the highest virus concentrations used in these studies (6 × 10e12 GC/mL), up to 20% of the cells in the ganglion cell layer were found to express the transgene. Interestingly, at the lowest virus concentration (1 × 10e10 GC/mL), the expression was targeted to AII amacrine cells.[41] A promoter was also found to target AII in another study but it is unclear how specific the targeting was.[42] Although these studies showed that it is possible to obtain weak expression in AII amacrine cells, the expression being also present in other cell types, finding a promoter to allow higher level expression in this target cell population was still needed to test a reactivation strategy based on AII amacrine cells.

Restoring the diversity of responses is important for restoring high-quality visual perception. Previous studies on the primate retina[14,17]

have shown that a selective impairment of retinal computations leads to specific deficits in visual perception. Inactivating ON cells in the macaque retina *in vivo* using pharmacology[17] affected the ability of the macaque to detect light increase but did not affect its ability to detect light decrease. Recent work looking at responses of mouse RGCs and behavior at scotopic light levels suggests that the mouse relies on the responses of ON RGCs to detect light increase, and on OFF RGCs to detect light decrease.[43] A striking finding was that mice engaged in a task where they had to detect light increase in darkness would not use the information available from OFF RGCs, even when they are more sensitive than ON RGCs.[43] This strongly suggests that ON RGCs are used to detect light increase and OFF RGCs to detect light decrease, at least in scotopic conditions. These studies suggest that targeting AII amacrine cells with optogenetics should allow blind mice to perform visual tasks that could not be achieved by mice where RGCs have been targeted. However, this is a hypothesis that remains to be tested.

These previous results suggest that restoring retinal computations might be necessary for a blind patient to perform complex visual tasks. Previous studies have proposed alternative strategies targeting either "dormant" cones[18] or bipolar cells.[44–49] In many retinal dystrophy patients, photoreceptors are not present in late stages, and bipolar cells can be partially degenerate.[50] Indeed, RGCs and AII amacrine cells have been shown to be the most robust neuronal cell types during retinal degeneration. AII amacrine cells that are stable over a longer time[51] can therefore be used at the most advanced stages of degeneration.

However, ultimately, these advantages will have to be evaluated in primate models to attest translational feasibility. It remains to be seen if the same level of expression and specificity found here can be achieved in primate models. Nevertheless, our results show that targeting AII for optogenetic stimulation is a promising new avenue for vision restoration. Other amacrine cell types that would also be able to evoke ON and OFF responses could also be promising targets that might be amenable to optogenetic therapy if adequate vector promoter combinations become available over time.

MATERIALS AND METHODS

AAV productions

Recombinant AAVs were produced by the plasmid cotransfection method, and the resulting lysates were purified via iodixanol gradient ultracentrifugation, as previously described.[27] Briefly, 40% iodixanol fraction was concentrated and buffer exchanged using Amicon Centrifugal Filter Units (Millipore, Molsheim, France). Vector stocks were then titrated for DNase-resistant vector genomes with ITR primers by real-time qPCR with SybrGreen (ThermoFischer Scientific) relative to a standard. Subcloning of plasmid constructs was performed by either Genscript (Rijswik, Netherlands) or Genecust (Boynes, France). Initially, while testing different opsins, eNphR3.0-TS-eYFP-ER-WPRE (a gift from Karl Deisseroth, Addgene plasmid #26966) replaced GFP in the plasmid construct. Later, the excitatory opsin ReaChR and inhibitory opsin GtACR1 (a gift from Peter Hegemann, Addgene plasmid #85464) replaced eNphR3.0 to create HKamac-ReachR-TS-eYFP- ER-WPRE and HKamac-GtACR1-TS-eYFP-ER-WPRE, respectively. These constructs, therefore, retain the trafficking and ER signals that were used to help membrane expression of eNphr3.0.[52]

Animals and intravitreal injections

All experiments were done in accordance with Directive 2010/63/EU of the European Parliament. The protocol was approved by the Local Animal Ethics Committee of Paris 5 (CEEA 34). All mice used in this study were C3H/FeJ (rd1 mice) or C57Bl6J mice (wild type) from Janvier Laboratories (Le Genest Saint Isle, France). For injections, mice were anesthetized with isoflurane (5% induction, 2% during the procedure). Pupils were dilated, and an ultrafine 30-gauge disposable needle was passed through the sclera, at the equator and next to the limbus, into the vitreous cavity. Injection of 1.5 μL stock containing 3e9 vg/eye of AAV-GFP or ReaChR-eYFP was made with direct observation of the needle in the center of the vitreous cavity.

Immunohistochemistry

Mice were euthanized in accordance with all animal facility protocols at the Institut de la Vision by CO_2 inhalation and cervical dislocation. Eyes were removed and fixed 2 h in 4% paraformaldehyde solution at room temperature. Eyes for flatmounts were dissected and retinal whole mounts were prepared for imaging. Eyes for sectioning were cryopreserved in 30% sucrose prior to embedding in OCT (Thermofisher, Waltham MA) and cut into 12-μm sections using a cryostat. Slides were washed for 10 min, blocked for 1 h in 6% NDS/1% BSA/0.5% Triton in PBS 1X, and incubated overnight in 50% block solution diluted in PBS with anti-Prox1 1:500 (Biolegend, San Diego, CA; Rb), anti-ChAT 1:1,000 (Chemicon, Gt), washed 3 × 5 min in PBS 1X, incubated with Alexa Fluor conjugated secondary antibody 1:1,000 and DAPI 1:2,000 for 1–2 h at room temperature, washed 3 × 5 min, and coverslipped in mounting medium (Vectashield). Images were then acquired using a confocal microscope and analyzed using Fiji by Z-stacking.

Multielectrode array

Multielectrode array (MEA) recordings were obtained from *ex vivo* isolated flat-mounted retinas of wild-type mice and rd1 mice aged from 132 to 324 days. Mice were euthanized by quick cervical dislocation, and eyeballs were removed and placed in Ames medium (Sigma-Aldrich, St Louis, MO; A1420) bubbled with 95% O_2 and 5% CO_2 at room temperature. Isolated retinas were placed on a cellulose membrane and gently pressed against an MEA (MEA256 iR-ITO; Multi-Channel Systems, Reutlingen, Germany), with the RGCs facing the electrodes. For wild-type and rd1 recordings, MEAs with respectively 3-μm and 60-μm electrode spacing were used. Pharmacology was used to block photoreceptor to bipolar cell transmission with 5 μm L-AP4 and 1 μm ACET, followed by 200 μm CNQX and 10 μm CPP in some experiments to block all transmission to RGCs (Tocris, Bristol UK). All of the multielectrode array recordings were processed with the software spyking-circus[53] to sort the recorded spikes and obtain templates of individual RGC responses.

Light stimulation

To study the responses of RGCs to optogenetic stimulation, we used a flickering stimulus (referred to as flicker in the following) consisting of a series of full-field flashes of 1-s duration, interleaved with 1-s intervals of darkness. Flashes were played both at low (41.6 μW cm^{-2}) and high (833 μW cm^{-2}) light intensities (see Sengupta et al.[7] for a similar intensity tuning for ReachR expressed in ganglion cells). To study the diversity of the cell responses, we used a chirp stimulus. This is a full-field stimulus, lasting 25 s, designed to test the reaction of ganglion cells to changes in light intensity at different regimes of contrast and frequency. After a 1-s flash, the light intensity varies at constant speed and increasing contrast for 10 s, and with constant contrast and increasing frequency for other 10 s. We used white light for all the wild-type experiments, and green light (550 nm) for the rd1 experiments, with a similar intensity. Output light intensities were calibrated by using a power meter (Thorlabs).

Detection of ganglion cell responses

To check if a stimulus **s** evoked a response in a given ganglion cell, we did the following test. First, we considered a control window of 300 ms right before the stimulus onset. For a given cell **c**, we calculated the average spontaneous firing rate $\mathbf{r_{ctrl}^{c,s}}$ and its standard deviation $\boldsymbol{\sigma}_{\mathbf{ctrl}}\mathbf{c,s}$ across repetitions in this time interval. We defined an activation threshold $\mathbf{T^{c,s}}$ as follows:

$$r_{ctrl}^{c,s} + max\left[5\sigma_{ctrl,}^{c,s} h\right]$$

With h equal to 10 Hz. Then, we looked at a response window of 300 ms after the presentation of the stimulus (specifically, right after the stimulus onset for ON responses, and after the stimulus offset for OFF responses), and computed the peri-stimulus time histogram $\mathbf{psth^{c,s}}$ of these responses (time bin equal to 50 ms). We considered that there was a response if the mean response $\mathbf{psth^{c,s}}$ exceeded the activation threshold $\mathbf{T^{c,s}}$.

Classification of ON and OFF ganglion cells

We used the criterion above to classify ON and OFF RGCs. We labeled as ON or OFF all the cells that responded respectively to the onset or to the offset of the flicker. Cells responding at both onset and offset were labeled as ON-OFF. Cells that were not responding at all were not labeled, and have not been considered in further analyses. For the excitatory opsin protocol (ReaChR), we pooled data from three different experiments, obtaining a total population of 173 ON, 65 OFF, and 44 ON-OFF ganglion cells. For the control protocol, we recorded from two different retinas, and identified a total of 113 ON, 94 OFF, and 51 ON-OFF ganglion cells. For the inhibitory opsin protocol (gtACR1), we collected data from a single experiment, and found 36 ON, 125 OFF, and 9 ON-OFF ganglion cells.

Analysis of RGC responses to optogenetic stimulation

To study the responses of RGCs to the optogenetic stimulation, we displayed the flicker at the same low and high light intensities as above. Then, for each luminance level, we calculated the percentage of ON and OFF cells with detectable responses at both stimulus onset and offset. We did the same analysis to test the impact of both the excitatory and inhibitory opsins (respectively ReaChR and gtACR1, Figures 2D, 3E, and 4C), and for all the control protocols with L-AP4, ACET, and CNQX and CPP (Figures 2E and 3F). For the control experiments on rd1 mice, since the photoreceptor responses were not available, we could not preliminarily classify the ganglion cells as ON or OFF. As a consequence, we computed the percentages of RGCs activated on the entire population of cells, without any subdivision based on polarity (Figure 6E).

Off-target expression of RGCs

To identify the RGCs directly expressing ReaChR due to the expression leakage, we looked at the optogenetic responses to the flicker after application of CNQX and CPP. We labeled as affected by the leakage all those cells for which a detectable response (either at stimulus onset and/or offset) was detectable. We did not consider these RGCs for the sustained-transient analysis nor for the complexity analysis described below.

Sustained-transient index

We defined a sustained-transient index $\mathbf{ST^{c,s}}$to assess which component is prevailing (transient or sustained) in the responses of a given ganglion cell **c** to a certain stimulus **s**. We considered two response windows subsequent to the presentation of the stimulus: a first one capturing transient responses (from 0 ms to 300 ms after stimulus onset for ON cells, and after stimulus offset for OFF cells) and a second one for sustained responses (from 300 ms to 600 ms after onset for ON cells and after offset for OFF cells). We computed the peri-stimulus time histogram of the responses (time bin equal to 50 ms) on both windows: $\mathbf{psth_{trans}^{c,s}}$ representing the transient component, and $\mathbf{psth_{sust}^{c,s}}$ representing the sustained component. We then computed the sustained-transient index $\mathbf{ST^{c,s}}$ as the following ratio:

$$ST^{c,s} = \frac{max\left[psth_{sust}^{c,s}\right]}{max\left[psth_{sust}^{c,s}\right] + max\left[psth_{trans}^{c,s}\right]}$$

An index $\mathbf{ST^{c,s}}$ close to 1 entails that the cell **c** produces a sustained response to the stimulus **s**. Conversely, an index close to 0 means the response is predominantly transient.

Sustained-transient analysis

We used the **ST** index defined above to compare the transience of RGC responses to photoreceptors and optogenetic stimulations respectively. For this analysis, we only considered cells with detectable responses to both the photoreceptor and optogenetic responses. We also excluded all the cells for which optogenetic responses showed a different polarity with respect to the photoreceptor responses, and all those cells affected by the expression leakage, leaving us with a total of 48 good cells. We then calculated the sustained-transient index described above for all cells in both optogenetic and photoreceptor responses, and compared the distribution of the index under the two conditions using the Wilcoxon rank-sum test. We found that, for

the population of ON ganglion cells, these two distributions are significantly different, with the responses to optogenetic stimulation being more sustained (the test rejects the null hypothesis that the two distributions have equal medians with p-val < 1e-5). For the population of OFF cells, we did not observe a significant difference among the two distributions (Figure 5B).

To consolidate this result at single cell level, we computed for each cell a comparative index **ΔST**, defined as the difference of the ST indices computed respectively on the photoreceptor and optogenetic responses.

$$\Delta ST^{c} = ST^{c,photo} - ST^{c,opto}$$

This index has value close to 0 if the photoreceptor and optogenetic responses are similar in transience, value close to 1 if the cell has an optogenetic response more transient with respect to its normal photoreceptor responses, and value close to −1 if its optogenetic responses are more sustained. We looked at the distribution of this index for both ON and OFF ganglion cells (Figure 5C), and observed that the vast majority of ON RGCs (31 cells out of 34) has a negative relative index, indicating that ON ganglion cells tend to lose their transient component when activated optogenetically through the AII pathway.

Analysis of complexity of the responses

To assess the complexity of RGC responses, we relied on PCA. We computed the principal components of the ganglion cell responses to the chirp stimulus for both photoreceptor and optogenetic stimulation, and compared the number of components needed to explain different percentages of variance. We applied the selection criteria used for the sustained-transient analysis described above: we only kept cells consistently responding to both photoreceptor and optogenetic stimulation, and excluded all the cells featuring off-target expression, for a total of 40 good cells. As we did not want to account for inter-experimental variability, we ran the analysis independently for each of the three experiments. To make the results comparable, we needed to keep the population size constant across the different experiments. As a consequence, we ran the PCA on each experiment on a sampled subpopulation of fixed size (30 cells). We repeated this procedure 100 times, and for each experiment we computed the average curve showing the variance explained by each number of principal components under both normal and optogenetic conditions (Figure 5E). We then obtained the final results by averaging the curves across all three experiments (opaque lines in Figure 5E).

DATA AND CODE AVAILABILITY

The code used in all our analysis is available online (www.github.com/jagorn/MEA-Analysis). The dataset used to generate the figures will be made available upon request.

SUPPLEMENTAL INFORMATION

Supplemental information can be found online at https://doi.org/10.1016/j.omtm.2023.09.003.

ACKNOWLEDGMENTS

We thank the Paris Vision Institute core facilities (Animal facility platform, Histology platform, Imaging platform) and particularly Camille Robert of the vector core facility for producing the AAVs. This work was supported ERC Starting Grant (REGNETHER 639888/DD), ERC Consolidator Grant (DEEPRETINA, 101045253), the Centre National de la Recherche Scientifique (CNRS), the Institut National de la Santé et de la Recherche Médicale (INSERM), AFM-Téléthon (PhD Fellowship H.K.), Foundation Fighting Blindness (PPA-0919-0772-INSERM), Sorbonne Université, LabEx LIFESENSES (ANR-10-LABX-65), IHU FOReSIGHT (ANR-18-IAHU-01), Paris Ile-de-France Region under « DIM Thérapie génique » initiative, Foundation Fighting Blindness (Program Project Award), ANR grants (ANR-18-CE37-0011 – DECORE, ANR-20-CE37-0018-04-Shooting Star, NUTRIACT, PerBaCo, RetNet4EC), AVIESAN-UNADEV (O.M.), and Retina France (O.M.). E.O. was supported by a fellowship from the Ecole des Neurosciences des Paris (ENP) Ile-de-France.

AUTHOR CONTRIBUTIONS

H.K., E.O., F.T., D.D., and O.M. designed the study. H.K. and E.O. performed the experiments with help from M.R. and M.D. E.O. and F.T. analyzed the data with help from P.Y. and O.M. H.K., E.O., F.T., D.D., and O.M. wrote the manuscript.

DECLARATION OF INTERESTS

D.D. reports grants from Foundation Fighting Blindness, USA and European Research Council, during the conduct of the study; D.D. is a co-inventor on patent #9193956 (Adeno-associated virus virions with variant capsid and methods of use thereof), with royalties paid to Adverum Biotechnologies. D.D. also has personal financial interests in Tenpoint Tx. and SparingVision, outside the submitted work. D.D., H.K., O.M., F.T., and E.O. are inventors on pending patent applications on methods to target A2 amacrine cells related to this work.

REFERENCES

1. Lorach, H., Benosman, R., Marre, O., Ieng, S.-H., Sahel, J.A., and Picaud, S. (2012). Artificial retina: the multichannel processing of the mammalian retina achieved with a neuromorphic asynchronous light acquisition device. J. Neural. Eng. *9*, 066004. https://doi.org/10.1088/1741-2560/9/6/066004.

2. da Cruz, L., Dorn, J.D., Humayun, M.S., Dagnelie, G., Handa, J., Barale, P.-O., Sahel, J.-A., Stanga, P.E., Hafezi, F., Safran, A.B., et al. (2016). Five-year safety and performance results from the Argus II retinal prosthesis system clinical trial. Ophthalmology *123*, 2248–2254. https://doi.org/10.1016/j.ophtha.2016.06.049.

3. Beyeler, M., Nanduri, D., Weiland, J.D., Rokem, A., Boynton, G.M., and Fine, I. (2019). A model of ganglion axon pathways accounts for percepts elicited by retinal implants. Sci. Rep. *9*, 9199. https://doi.org/10.1038/s41598-019-45416-4.

4. Ferrari, U., Deny, S., Sengupta, A., Caplette, R., Trapani, F., Sahel, J.-A., Dalkara, D., Picaud, S., Duebel, J., and Marre, O. (2020). Towards optogenetic vision restoration with high resolution. PLoS Comput. Biol. *16*, e1007857. https://doi.org/10.1371/journal.pcbi.1007857.

5. Bi, A., Cui, J., Ma, Y.-P., Olshevskaya, E., Pu, M., Dizhoor, A.M., and Pan, Z.-H. (2006). Ectopic expression of a microbial-type rhodopsin restores visual responses in mice with photoreceptor degeneration. Neuron *50*, 23–33. https://doi.org/10.1016/j.neuron.2006.02.026.

6. Caporale, N., Kolstad, K.D., Lee, T., Tochitsky, I., Dalkara, D., Trauner, D., Kramer, R., Dan, Y., Isacoff, E.Y., and Flannery, J.G. (2011). LiGluR restores visual responses

in rodent models of inherited blindness. Mol. Ther. *19*, 1212–1219. https://doi.org/10.1038/mt.2011.103.

7. Sengupta, A., Chaffiol, A., Macé, E., Caplette, R., Desrosiers, M., Lampič, M., Forster, V., Marre, O., Lin, J.Y., Sahel, J.-A., et al. (2016). Red-shifted channelrhodopsin stimulation restores light responses in blind mice, macaque retina, and human retina. EMBO Mol. Med. *8*, 1248–1264. https://doi.org/10.15252/emmm.201505699.

8. Chaffiol, A., Caplette, R., Jaillard, C., Brazhnikova, E., Desrosiers, M., Dubus, E., Duhamel, L., Macé, E., Marre, O., Benoit, P., et al. (2017). A new promoter allows optogenetic vision restoration with enhanced sensitivity in macaque retina. Mol. Ther. *25*, 2546–2560. https://doi.org/10.1016/j.ymthe.2017.07.011.

9. Berry, M.H., Holt, A., Salari, A., Veit, J., Visel, M., Levitz, J., Aghi, K., Gaub, B.M., Sivyer, B., Flannery, J.G., and Isacoff, E.Y. (2019). Restoration of high-sensitivity and adapting vision with a cone opsin. Nat. Commun. *10*, 1221. https://doi.org/10.1038/s41467-019-09124-x.

10. Sahel, J.-A., Boulanger-Scemama, E., Pagot, C., Arleo, A., Galluppi, F., Martel, J.N., Esposti, S.D., Delaux, A., de Saint Aubert, J.-B., de Montleau, C., et al. (2021). Partial recovery of visual function in a blind patient after optogenetic therapy. Nat. Med. *27*, 1223–1229. https://doi.org/10.1038/s41591-021-01351-4.

11. Sanes, J.R., and Masland, R.H. (2015). The types of retinal ganglion cells: current status and implications for neuronal classification. Annu. Rev. Neurosci. *38*, 221–246. https://doi.org/10.1146/annurev-neuro-071714-034120.

12. Baden, T., Berens, P., Franke, K., Román Rosón, M., Bethge, M., and Euler, T. (2016). The functional diversity of retinal ganglion cells in the mouse. Nature *529*, 345–350. https://doi.org/10.1038/nature16468.

13. Deny, S., Ferrari, U., Macé, E., Yger, P., Caplette, R., Picaud, S., Tkačik, G., and Marre, O. (2017). Multiplexed computations in retinal ganglion cells of a single type. Nat. Commun. *8*, 1964. https://doi.org/10.1038/s41467-017-02159-y.

14. Merigan, W.H., Byrne, C.E., and Maunsell, J.H. (1991). Does primate motion perception depend on the magnocellular pathway? J. Neurosci. *11*, 3422–3429. https://doi.org/10.1523/jneurosci.11-11-03422.1991.

15. Yonehara, K., Fiscella, M., Drinnenberg, A., Esposti, F., Trenholm, S., Krol, J., Franke, F., Scherf, B.G., Kusnyerik, A., Müller, J., et al. (2016). Congenital nystagmus gene FRMD7 is necessary for establishing a neuronal circuit asymmetry for direction selectivity. Neuron *89*, 177–193. https://doi.org/10.1016/j.neuron.2015.11.032.

16. Hillier, D., Fiscella, M., Drinnenberg, A., Trenholm, S., Rompani, S.B., Raics, Z., Katona, G., Juettner, J., Hierlemann, A., Rozsa, B., and Roska, B. (2017). Causal evidence for retina-dependent and -independent visual motion computations in mouse cortex. Nat. Neurosci. *20*, 960–968. https://doi.org/10.1038/nn.4566.

17. Schiller, P.H., Sandell, J.H., and Maunsell, J.H. (1986). Functions of the ON and OFF channels of the visual system. Nature *322*, 824–825. https://doi.org/10.1038/322824a0.

18. Busskamp, V., Duebel, J., Balya, D., Fradot, M., Viney, T.J., Siegert, S., Groner, A.C., Cabuy, E., Forster, V., Seeliger, M., et al. (2010). Genetic reactivation of cone photoreceptors restores visual responses in retinitis pigmentosa. Science *329*, 413–417. https://doi.org/10.1126/science.1190897.

19. Famiglietti, E.V., Jr., and Kolb, H. (1975). A bistratified amacrine cell and synaptic circuitry in the inner plexiform layer of the retina. Brain Res. *84*, 293–300. https://doi.org/10.1016/0006-8993(75)90983-x.

20. Vaney, D.I. (1985). The morphology and topographic distribution of AII amacrine cells in the cat retina. Proc. Roy. Soc. Lond. *224*, 475–488. https://doi.org/10.1098/rspb.1985.0045.

21. Kolb, H., Linberg, K.A., and Fisher, S.K. (1992). Neurons of the human retina: a Golgi study. J. Comp. Neurol. *318*, 147–187. https://doi.org/10.1002/cne.903180204.

22. Wässle, H., Grünert, U., Chun, M.H., and Boycott, B.B. (1995). The rod pathway of the macaque monkey retina: identification of AII-amacrine cells with antibodies against calretinin. J. Comp. Neurol. *361*, 537–551. https://doi.org/10.1002/cne.903610315.

23. Xin, D., and Bloomfield, S.A. (1999). Comparison of the responses of AII amacrine cells in the dark- and light-adapted rabbit retina. Vis. Neurosci. *16*, 653–665. https://doi.org/10.1017/s0952523899164058.

24. Tsukamoto, Y., and Omi, N. (2017). Classification of mouse retinal bipolar cells: Type-specific connectivity with special reference to rod-driven AII amacrine pathways. Front. Neuroanat. *11*, 92. https://doi.org/10.3389/fnana.2017.000.

25. Kolb, H., and Nelson, R. (1983). Rod pathways in the retina of the cat. Vis. Res. *23*, 301–312. https://doi.org/10.1016/0042-6989(83)90078-0.

26. Strettoi, E., Raviola, E., and Dacheux, R.F. (1992). Synaptic connections of the narrow-field, bistratified rod amacrine cell (AII) in the rabbit retina. J. Comp. Neurol. *325*, 152–168. https://doi.org/10.1002/cne.903250203.

27. Dalkara, D., Byrne, L.C., Klimczak, R.R., Visel, M., Yin, L., Merigan, W.H., Flannery, J.G., and Schaffer, D.V. (2013). In vivo-directed evolution of a new adeno-associated virus for therapeutic outer retinal gene delivery from the vitreous. Sci. Transl. Med. *5*, 189ra76. https://doi.org/10.1126/scitranslmed.3005708.

28. Khabou, H., Garita-Hernandez, M., Chaffiol, A., Reichman, S., Jaillard, C., Brazhnikova, E., Bertin, S., Forster, V., Desrosiers, M., Winckler, C., et al. (2018). Noninvasive gene delivery to foveal cones for vision restoration. JCI Insight *3*, e96029. https://doi.org/10.1172/jci.insight.96029.

29. Yokoyama, T., Liou, G.I., Caldwell, R.B., and Overbeek, P.A. (1992). Photoreceptor-specific activity of the human interphotoreceptor retinoid-binding protein (IRBP) promoter in transgenic mice. Exp. Eye Res. *55*, 225–233. https://doi.org/10.1016/0014-4835(92)90186-v.

30. Liou, G.I., Matragoon, S., Yang, J., Geng, L., Overbeek, P.A., and Ma, D.-P. (1991). Retina-specific expression from the IRBP promoter in transgenic mice is conferred by 212 bp of the 5′-flanking region. Biochem. Biophys. Res. Commun. *181*, 159–165. https://doi.org/10.1016/s0006-291x(05)81395-6.

31. Ying, S., Fong, S.L., Fong, W.B., Kao, C.W., Converse, R.L., and Kao, W.W. (1998). A CAT reporter construct containing 277bp GNAT2 promoter and 214bp IRBP enhancer is specifically expressed by cone photoreceptor cells in transgenic mice. Curr. Eye Res. *17*, 777–782. https://doi.org/10.1076/ceyr.17.8.777.5158.

32. Yeh C.Y. (2013). ARVO Annual Meeting (Seattle, WA), 2013; p. abstract 1937.30.

33. Ye, G.-J., Budzynski, E., Sonnentag, P., Nork, T.M., Sheibani, N., Gurel, Z., Boye, S.L., Peterson, J.J., Boye, S.E., Hauswirth, W.W., and Chulay, J.D. (2016). Cone-specific promoters for gene therapy of achromatopsia and other retinal diseases. Hum. Gene Ther. *27*, 72–82. https://doi.org/10.1089/hum.2015.130.

34. Helmstaedter, M., Briggman, K.L., Turaga, S.C., Jain, V., Seung, H.S., and Denk, W. (2013). Connectomic reconstruction of the inner plexiform layer in the mouse retina. Nature *500*, 168–174. https://doi.org/10.1038/nature12346.

35. Pérez de Sevilla Müller, L., Azar, S.S., de los Santos, J., and Brecha, N.C. (2017). Prox1 is a marker for AII amacrine cells in the mouse retina. Front. Neuroanat. *11*, 39. https://doi.org/10.3389/fnana.2017.00039.

36. Gauvain, G., Akolkar, H., Chaffiol, A., Arcizet, F., Khoei, M.A., Desrosiers, M., Jaillard, C., Caplette, R., Marre, O., Bertin, S., et al. (2021). Optogenetic therapy: high spatiotemporal resolution and pattern discrimination compatible with vision restoration in non-human primates. Commun. Biol. *4*, 125. https://doi.org/10.1038/s42003-020-01594-w.

37. Govorunova, E.G., Sineshchekov, O.A., Janz, R., Liu, X., and Spudich, J.L. (2015). NEUROSCIENCE. Natural light-gated anion channels: A family of microbial rhodopsins for advanced optogenetics. Science *349*, 647–650. https://doi.org/10.1126/science.aaa7484.

38. Wietek, J., Broser, M., Krause, B.S., and Hegemann, P. (2016). Identification of a natural green light absorbing chloride conducting channelrhodopsin from Proteomonas sulcata. J. Biol. Chem. *291*, 4121–4127. https://doi.org/10.1074/jbc.M115.699637.

39. Marc, R.E., and Jones, B.W. (2003). Retinal remodeling in inherited photoreceptor degenerations. Mol. Neurobiol. *28*, 139–148. 28:2:139. https://doi.org/10.1385/MN.

40. Guadagni, V., Biagioni, M., Novelli, E., Aretini, P., Mazzanti, C.M., and Strettoi, E. (2019). Rescuing cones and daylight vision in retinitis pigmentosa mice. FASEB J *33*, 10177–10192. https://doi.org/10.1096/fj.201900414R.

41. Ivanova, E., and Pan, Z.-H. (2009). Evaluation of the adeno-associated virus mediated long-term expression of channelrhodopsin-2 in the mouse retina. Mol. Vis. *15*, 1680–1689.

42. Jüttner, J., Szabo, A., Gross-Scherf, B., Morikawa, R.K., Rompani, S.B., Hantz, P., Szikra, T., Esposti, F., Cowan, C.S., Bharioke, A., et al. (2019). Targeting neuronal and glial cell types with synthetic promoter AAVs in mice, non-human primates

and humans. Nat. Neurosci. *22*, 1345–1356. https://doi.org/10.1038/s41593-019-0431-2.

43. Smeds, L., Takeshita, D., Turunen, T., Tiihonen, J., Westö, J., Martyniuk, N., Seppänen, A., and Ala-Laurila, P. (2019). Paradoxical rules of spike train decoding revealed at the sensitivity limit of vision. Neuron *104*, 576–587.e11. https://doi.org/10.1016/j.neuron.2019.08.005.

44. Lagali, P.S., Balya, D., Awatramani, G.B., Münch, T.A., Kim, D.S., Busskamp, V., Cepko, C.L., and Roska, B. (2008). Light-activated channels targeted to ON bipolar cells restore visual function in retinal degeneration. Nat. Neurosci. *11*, 667–675. https://doi.org/10.1038/nn.2117.

45. Cronin, T., Vandenberghe, L.H., Hantz, P., Juttner, J., Reimann, A., Kacsó, A.E., Huckfeldt, R.M., Busskamp, V., Kohler, H., Lagali, P.S., et al. (2014). Efficient transduction and optogenetic stimulation of retinal bipolar cells by a synthetic adeno-associated virus capsid and promoter. EMBO Mol. Med. *6*, 1175–1190. https://doi.org/10.15252/emmm.201404077.

46. Macé, E., Caplette, R., Marre, O., Sengupta, A., Chaffiol, A., Barbe, P., Desrosiers, M., Bamberg, E., Sahel, J.-A., Picaud, S., et al. (2015). Targeting channelrhodopsin-2 to ON-bipolar cells with vitreally administered AAV Restores ON and OFF visual responses in blind mice. Mol. Ther. *23*, 7–16. https://doi.org/10.1038/mt.2014.154.

47. Gaub, B.M., Berry, M.H., Holt, A.E., Isacoff, E.Y., and Flannery, J.G. (2015). Optogenetic vision restoration using rhodopsin for enhanced sensitivity. Mol. Ther. *23*, 1562–1571. https://doi.org/10.1038/mt.2015.121.

48. van Wyk, M., Pielecka-Fortuna, J., Löwel, S., and Kleinlogel, S. (2015). Restoring the ON switch in blind retinas: Opto-mGluR6, a next-generation, cell-tailored optogenetic tool. PLoS Biol. *13*, e1002143. https://doi.org/10.1371/journal.pbio.1002143.

49. Cehajic-Kapetanovic, J., Eleftheriou, C., Allen, A.E., Milosavljevic, N., Pienaar, A., Bedford, R., Davis, K.E., Bishop, P.N., and Lucas, R.J. (2015). Restoration of vision with ectopic expression of human rod opsin. Curr. Biol. *25*, 2111–2122. https://doi.org/10.1016/j.cub.2015.07.029.

50. Francis, P.J., Mansfield, B., and Rose, S. (2013). Proceedings of the first International Optogenetic Therapies for vision symposium. Transl. Vis. Sci. Technol. *2*, 4. https://doi.org/10.1167/tvst.2.7.4.

51. Strettoi, E., Porciatti, V., Falsini, B., Pignatelli, V., and Rossi, C. (2002). Morphological and functional abnormalities in the inner retina of the rd/rd mouse. J. Neurosci. *22*, 5492–5504. https://doi.org/10.1523/jneurosci.22-13-05492.2002.

52. Gradinaru, V., Zhang, F., Ramakrishnan, C., Mattis, J., Prakash, R., Diester, I., Goshen, I., Thompson, K.R., and Deisseroth, K. (2010). Molecular and cellular approaches for diversifying and extending optogenetics. Cell *141*, 154–165. https://doi.org/10.1016/j.cell.2010.02.037.

53. Yger, P., Spampinato, G.L., Esposito, E., Lefebvre, B., Deny, S., Gardella, C., Stimberg, M., Jetter, F., Zeck, G., Picaud, S., et al. (2018). A spike sorting toolbox for up to thousands of electrodes validated with ground truth recordings in vitro and in vivo. Elife *7*, e34518. https://doi.org/10.7554/elife.34518.